J. Membrane Biol. 150, 47–62 (1996)

The Journal of
Membrane
Biology

A Novel, Volume-correlated Cl^- Conductance in Marginal Cells Dissociated from the Stria Vascularis of Gerbils

S. Takeuchi, A. Irimajiri
Department of Physiology, Kochi Medical School, Nankoku 783, Japan

Received: 15 August 1995/Revised: 3 November 1995

Abstract. Using the whole-cell patch-clamp technique, we examined Cl^--selective currents manifested by strial marginal cells isolated from the inner ear of gerbils. A large Cl^--selective conductance of ~18 nS/pF was found from nonswollen cells in isotonic buffer containing 150 mM Cl^-. Under a quasi-symmetrical Cl^- condition, the 'instantaneous' current-voltage relation was close to linear, while the current-voltage relation obtained at the end of command pulses of duration 400 msec showed weak outward rectification. The permeability sequence for anionic currents was as $SCN^- > Br^- \cong Cl^- > F^- > NO_3^- \cong I^- > gluconate^-$, corresponding to Eisenmann's sequence V. When whole-cell voltage clamped in isotonic bathing solutions, the cells exhibited volume changes that were accounted for by the Cl^- currents driven by the imposed electrochemical potential gradients. The volume change was elicited by lowered extracellular Cl^- concentration, anion substitution and altered holding potentials. The Cl^- conductance varied in parallel with cell volume when challenged by bath anisotonicity. The whole-cell Cl^- current was only partially blocked by both 5-nitro-2-(3-phenylpropylamino) benzoic acid (NPPB, 0.5 mM) and diphenylamine-2-carboxylic acid (DPC, 1.0 mM), but 4-acetamido-4′-isothiocyanato-stilbene-2,2′-disulfonic acid (SITS, 0.5 mM) was without effect. The properties of the present whole-cell Cl^- current resembled those of the single Cl^- channel previously found in the basolateral membrane of the marginal cell (Takeuchi et al., *Hearing Res.* **83:**89–100, 1995), suggesting that the volume-correlated Cl^- conductance could be ascribed predominantly to the basolateral membrane. This Cl^- conductance may function not only in cell volume regulation but also for the transport of Cl^- and the setting of membrane potential in marginal cells under physiological conditions.

Key words: Chloride conductance — Cell volume — Marginal cell — Endolymph — Inner ear

Introduction

The endolymph in the cochlea is unique and without a true counterpart in any other variety of extracellular fluids. Its predominant cation is K^+ in place of Na^+ and its electrical potential (endocochlear potential, EP) is positive by ~80 mV relative to the perilymph (Johnstone & Sellick, 1972). As the major site responsible for producing such a unique situation in the inner ear of mammals, the marginal cells of the stria vascularis, in particular, have been implicated and thereby highlighted for their transport properties. Recently, several groups, all employing the patch clamp single-channel recording technique, have reported the presence in marginal cells of the following ion channels. From the *apical* membrane: (i) nonselective cation channels (Takeuchi, Marcus & Wangemann, 1992; Sunose et al., 1993), (ii) small-conductance K^+ channels (Sunose et al., 1994), and (iii) 12-pS Cl^- channels during stimulation by cyclic AMP (Sunose et al., 1993); from the *basolateral* membrane: (iv) nonselective cation channels (Takeuchi et al., 1995) and (v) 80-pS Cl^- channels (Takeuchi et al., 1995).

We have developed a technique for obtaining single, viable strial cells suitable for physiological studies (Takeuchi et al., 1995) and have now applied the whole-cell recording technique to those single cells. In this first report on the whole-cell conductance of marginal cells, we focus on the Cl^- conductance for the following reasons: (i) a large contribution of Cl^- conductance to membrane potential has been reported of the vestibular dark

Correspondence to: S. Takeuchi

Table 1. Composition of solutions (in mM)

Solution	A	B	C	D	E	F	G	H	I	J	K
NMDG-Cl	140				150	50	15	150	150	75	75
NaCl		150	150								
NaX*				150							
$MgCl_2$	1	1	1								
$MgSO_4$				1	1	1	1	1	1	1	1
$CaCl_2$			0.7								
HEPES	6										
Tris	6										
K_2HPO_4		1.6	1.6	1.6	1.6	1.6	1.6	1.6	1.6	1.6	1.6
KH_2PO_4		0.4	0.4	0.4	0.4	0.4	0.4	0.4	0.4	0.4	0.4
EGTA	1	1									
ATP-Na_2	1										
Glucose		5	5	5	5	5	5	5	5	5	5
Mannitol						172	234	75	150	132	
Osmolality** (mOsm/kg)	274	293	290	280~296	290	289	287	368	448	290	148

* X = Cl^-, SCN^-, Br^-, F^-, I^-, NO_3^- or gluconate$^-$. The pHs are 7.2 for solution A (pipette) and 7.4 for others (bath). ** Measured by freezing point osmometry

cell, an analogous cell in the vestibular system (Wangemann & Marcus, 1992), (ii) 80-pS Cl^- channels have already been found, at a relatively high density, in the basolateral membrane of marginal cells (Takeuchi et al., 1995), and (iii) Cl^- channels play an important role in K^+ secretion by the strial marginal cell (Wangemann, Liu & Marcus, 1995).

Some of known epithelial channels for Cl^- are cell volume sensitive and swelling-induced activation of these channels strongly indicates their pivotal role in the mechanism of regulatory volume decrease (Worrell et al., 1989; McCann, Li & Welsh, 1989; Kubo & Okada, 1992; Chan et al., 1993). For the marginal cell, however, there has been no attempt to disclose any volume regulatory mechanism(s) operating in it. It is highly likely that volume-sensitive Cl^- channels, if any, substantially contribute to volume regulation in this cell type also. Thus the aim of the present study is to characterize the properties of Cl^- conductance with special attention paid to its relevance to volume changes of the marginal cell. A preliminary account of this work has appeared (Takeuchi & Irimajiri, 1995).

Materials and Methods

Cell Preparation

Marginal cells were prepared from the inner ear of gerbils as described previously (Takeuchi et al., 1995). Briefly, tissue strips (~2 mm long) from the stria vascularis freed of the underlying ligament were transferred to solution B (150 mM NaCl based, Ca^{2+}-free; for composition, *see* Table 1) containing 0.2% papain and incubated for 20 min at 23–25°C. These strips were then dissected with fine needles, under visual control, to obtain single marginal cells that retained their characteristic morphology: (i) a flat hexagonal apical surface, (ii) flourishing basal infoldings and (iii) an apically located nucleus. Morphologically acceptable cells thus selected also cleared the viability test based on dye exclusion (Takeuchi et al., 1995).

Estimation of Cell Volume

In most of the patch clamp experiments, the cell shape was simultaneously monitored at high magnification (1,000×) and its changes were recorded by a video monitor system. The test cell was held at the center of the field by means of the patch pipette. Thus we observed the cell's profile only. Dimensional measurements were done using an image processor (Argus 10, Hamamatsu Photonics, Hamamatsu, Japan). Changes in cell volume appeared most markedly in cell width leaving cell height almost unchanged (Fig. 1*A* & *D*). The width of a basal process in focus changed proportionally to that of cell trunk in several different experimental conditions (Fig. 1*C*). Accordingly, we estimated changes in relative cell volume v/v_c (here, v is volume and subscript c denotes 'control') from measurement of the widths of cell trunk (w_c and w) at three separate sections of a test cell in both control and experimental conditions, as illustrated in Fig. 1*B*. By assuming a relative invariance in cell height (h_c and h; *see* Fig. 1*D*), the v/v_c may be written as

$$v/v_c = (\bar{w}/\bar{w}_c)^2, \quad (1)$$

where $\bar{w}_c = (w_{c1} + w_{c2} + w_{c3})/3$ and $\bar{w} = (w_1 + w_2 + w_3)/3$.

Electrophysiology

The whole-cell configuration of the patch clamp technique (Marty & Neher, 1983) was used with pipettes of 3-5 MΩ when filled with solution A (140 mM NMDG-Cl based, Ca^{2+}-free; *see* Table 1). The use of pipettes of resistances below 3 MΩ resulted in a prohibitingly low rate of successful seals. Recordings were made with an amplifier (model 3900, Dagan, Minneapolis, MN) equipped with a model 3911 whole-cell expander. Electronic compensations were made for pipette

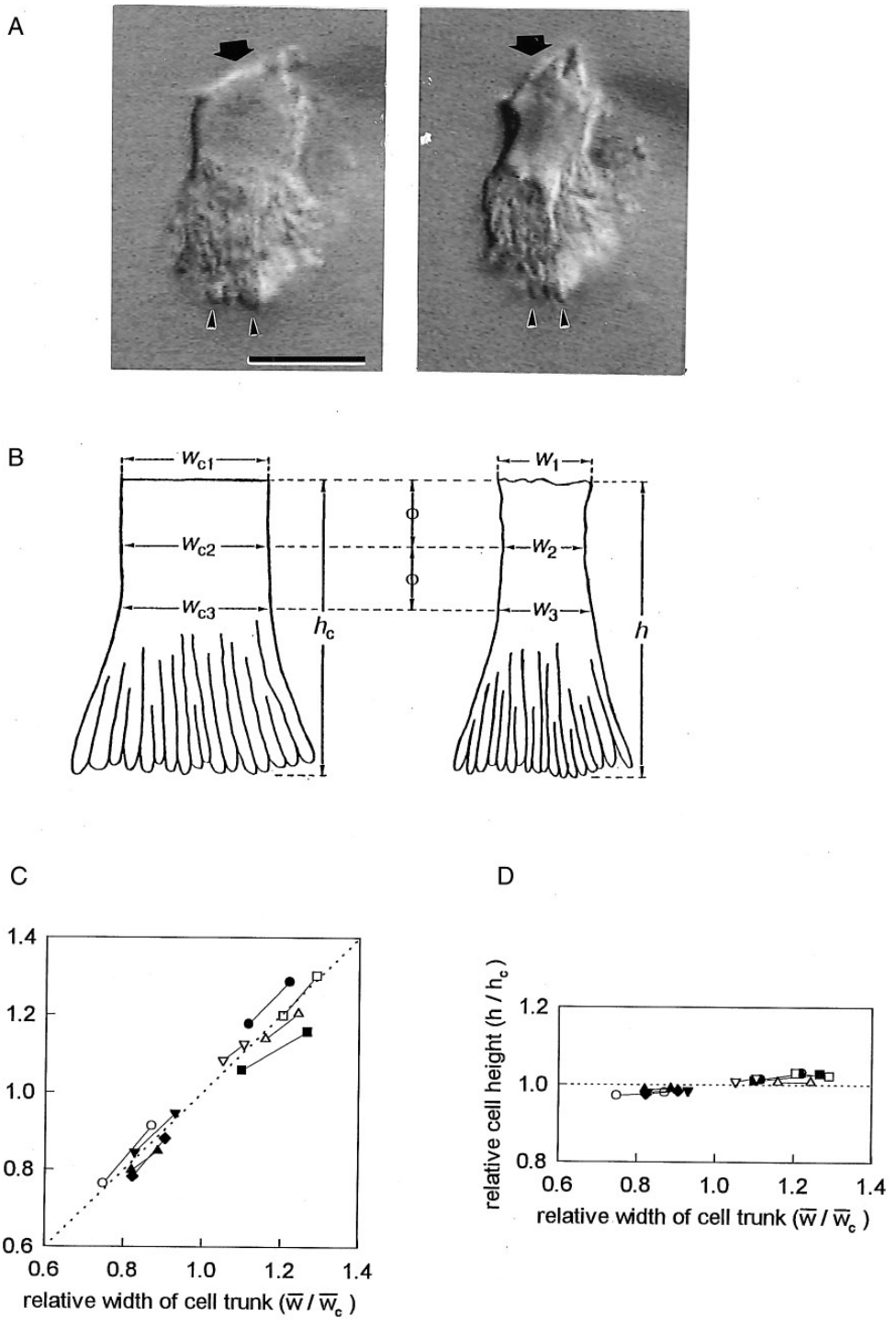

Fig. 1. Estimation of cell volume changes. (*A*) Video-microscopic profiles for a voltage-clamped marginal cell, with its apical membrane (*arrows*) upward and basal infoldings downward, before (*left*) and after (*right*) shrinkage due to anion replacement. The cell was bathed in solution D (Table 1) with $X = Cl^-$ (*left*) or $gluconate^-$ (*right*). Scale bar, 10 μm. Note parallel changes in width for both cell trunk and basal processes (*arrowheads*) when viewed in sharp focus. (*B*) Schematic drawings of the cell in (*A*) with the definition of size parameters included. (*C*) Correlation between the rate of change in width for cell trunk and that for basal process. Volume perturbation was effectuated by osmotic challenge, anion replacement, or alteration of holding potential. Relative widths for basal processes were measured as for the cell trunk. Different symbols indicate data from separate cells. Paired symbols interconnected by a line represent two determinations repeated at appropriate intervals following the volume perturbation, one being from the cell at the steady state. Mean slope of connecting lines, 1.02 ± 0.04 ($N = 9$). (*D*) Similar plots demonstrating poor correlation between changes in cell height and in cell width. Mean slope of connecting lines, 0.11 ± 0.01 ($N = 9$).

capacitances (3–4 pF), cell membrane capacitances (4–7 pF) and series resistances (5–15 MΩ), but not for leakage current components. Most experiments, unless otherwise noted, were performed in the voltage-clamp mode with the holding potential set at 0 mV before correction for liquid junction potentials. When solution J or K (75 mM NMDG-Cl based; *see* Table 1) was used in osmotic challenge experiments, the holding potential was set at the equilibrium potential for Cl^- (i.e., 16 mV). The bath solution was electrically connected to a Ag-AgCl electrode via a bridge of solution C (150 mM NaCl based; *see* Table 1). Membrane potentials were corrected for liquid junction potentials as reported (Takeuchi et al., 1995). The bath (~0.1 ml) was constantly perfused at 1.5 ml min^{-1} and maintained at room temperature (23–25°C). We employed the following two voltage-command protocols. One was a set of 0.4-sec pulse voltages varied, in 20-mV steps, between ±80 mV (Fig. 2*A*, *top*) and the other a ramp-voltage command swept from −80 to +80 mV in 1 sec (Fig. 2*D*, *top*). In time-chase experiments, ramp-voltage commands were applied at intervals of 3 sec. Voltage-command generation and data acquisition were both performed using pCLAMP software (version 5.7.1, Axon Instruments, Foster City, CA).

Analysis

Fitting quadratic curves to either of the 'instantaneous' currents defined at 10 msec after the onset of a command pulse and the 'quasi-steady' currents recorded at the end of the pulse, we obtained the respective current-voltage (*I-V*) relationships, from which the reversal voltage (E_{rev}), slope conductance (G) at 0 mV, and current (I) at −75 mV were determined. For *I-V* relations from the ramp-voltage command protocol, we determined the mean value of the slope conductance by a linear fit.

In the analysis of data from 'asymmetric' solution conditions, we have introduced the ratio I/I_{GHK} (I is the recorded current and I_{GHK} is the predicted current) for $V = -75$ mV as a measure of changes in the whole-cell Cl^- conductance. The quasi-steady current I was measured at a clamp voltage of −75 mV with solution A (140 mM NMDG-Cl based) inside the pipette. The magnitude of I_{GHK} was estimated on the basis of the Goldman-Hodgkin-Katz (GHK) current equation of the form:

$$I = \sum_i \frac{z_i^2 F^2 V}{RT} P_i \frac{X_i^b - X_i^p \exp(z_i FV/RT)}{1 - \exp(z_i FV/RT)} \quad (2)$$

where z, F, R and T have their usual meaning, P_i is the permeability to ion i, V the voltage across the membrane and X_i the concentration of ion i in the bath (b) or pipette (p). Assuming that P_{Cl} was the same as that under the control condition ($[Cl^-]_{bath}$ = 150 mM), the prediction of I_{GHK} for a reduced $[Cl^-]_{bath}$ was made as follows. The value of P_{Cl} corresponding to the I measured with $V = -75$ mV and X^b_{Cl} = 150 mM was first determined; putting this P_{Cl} value in Eq. (2) together with $V = -75$ mV and X^b_{Cl} = 50 mM, for instance, yielded the I_{GHK} predictable for this particular condition. The I_{GHK} for the bi-ionic condition (e.g., X^b_{Br} = 150 mM *vs.* X^p_{Cl} = 140 mM) was computed as follows. P_{Cl} was assumed to be the same as that for the quasi-symmetric Cl^- condition for $V = -75$ mV; P_{Br} was then calculated using the permeability ratio P_{Br}/P_{Cl} derived from the respective reversal potentials E_{rev}s (Table 2); and putting these P values in Eq. (2) together with $V = -75$ mV and pertinent X^bs yielded the I_{GHK} predicted.

The rationale for the above procedure came from the following inferences. For an anion-selective membrane, it is expected from Eq. (2) that currents driven by large negative membrane potentials (e.g., −75 mV) should depend primarily on the intracellular anion concentration (X^p_{Cl} = 140 mM in this study) as well as on the permeability to intracellular anion species since the exponential term in Eq. (2) amounted to ~18 for $z_i = -1$, $V = -75$ mV and T = 23–25°C. Likewise, the I_{GHK} under a bi-ionic condition such as X^b_{Br} = 150 mM *vs.* X^p_{Cl} = 140 mM should also depend mainly on P_{Cl} since from Eq. (2) it follows that I_{GHK} (and I also) $\propto P_{Cl} - 0.06\, P_{Br}$. Thus, the deviation of I/I_{GHK} from unity can be regarded as due mainly to the change in P_{Cl}.

Data are expressed as means ± SEM (N, number of cells). Curve fittings were done by the least-squares method. Data from one typical cell are presented after confirmation of similar results from four separate cells at least. Statistical analyses were made by Student's *t*-test with 95% confidence level.

Solutions and Chemicals

The composition of solutions used is given in Table 1. The pipettes were filled with solution A (140 mM NMDG-Cl based, Ca^{2+}-free, and with 1 mM ATP) throughout. Solution B (150 mM NaCl based, Ca^{2+}-free) was used for cell preparation. Giga-seals were formed in solution C (150 mM NaCl based). Anion selectivity was investigated with solution D. Bath Cl^- concentrations were isosmotically varied by using solutions E (150 mM), F (50 mM) and G (15 mM). Blockers were directly dissolved in solution E, just prior to use, under a vigorous stirring for up to 90 min, and the pH was readjusted to 7.4 whenever necessary. Solutions H (368 mOsm/kg) and I (448 mOsm/kg) were prepared by supplementing solution E (150 mM NMDG-Cl based) with mannitol. Solution K (148 mOsm/kg) was made by omission of mannitol from solution J (75 mM NMDG-Cl based, 290 mOsm/kg).

N-methyl-D-glucamine (NMDG), ATP (disodium salt) and 4-acetamido-4′-isothiocyanato-stilbene-2,2′-disulfonic acid (SITS) came from Sigma (St. Louis, MO). Papain and diphenylamine-2-carboxylic acid (DPC) were from Wako Pure Chemical Industries (Osaka, Japan). 5-Nitro-2-(3-phenyl-propylamino)-benzoate (NPPB) was a generous gift from Hoechst Pharmaceutical Company (Frankfurt, Germany). Other chemicals were of analytical reagent grade from Nacalai Tesque (Kyoto, Japan).

Results

Whole-Cell Current Under Quasi-symmetric Solution Condition

With 140 mM NMDG-Cl (solution A) in the pipette and 150 mM NMDG-Cl (solution E) in the bath, both outward and inward currents were recorded in response to pulse voltages not exceeding ±80 mV (Fig. 2*A*). These currents observed immediately following the whole-cell clamp condition were accompanied by no appreciable changes in cell volume. The *I-V* relationships for instantaneous current were close to linear while those for quasi-steady-state current showed weak outward rectification (Fig. 2*B*). From data for quasi-steady-state current the slope conductance G at 0 mV and reversal potential E_{rev} were calculated to be 102.8 ± 8.3 nS (or ~18 nS/pF, when normalized with respect to membrane capacitance) and −0.4 ± 0.5 mV (N = 23), both being statistically not different from values for the instantaneous current (*not shown*). The *I-V* curve for data from a ramp-voltage command was virtually linear (Fig. 2D, *control*)

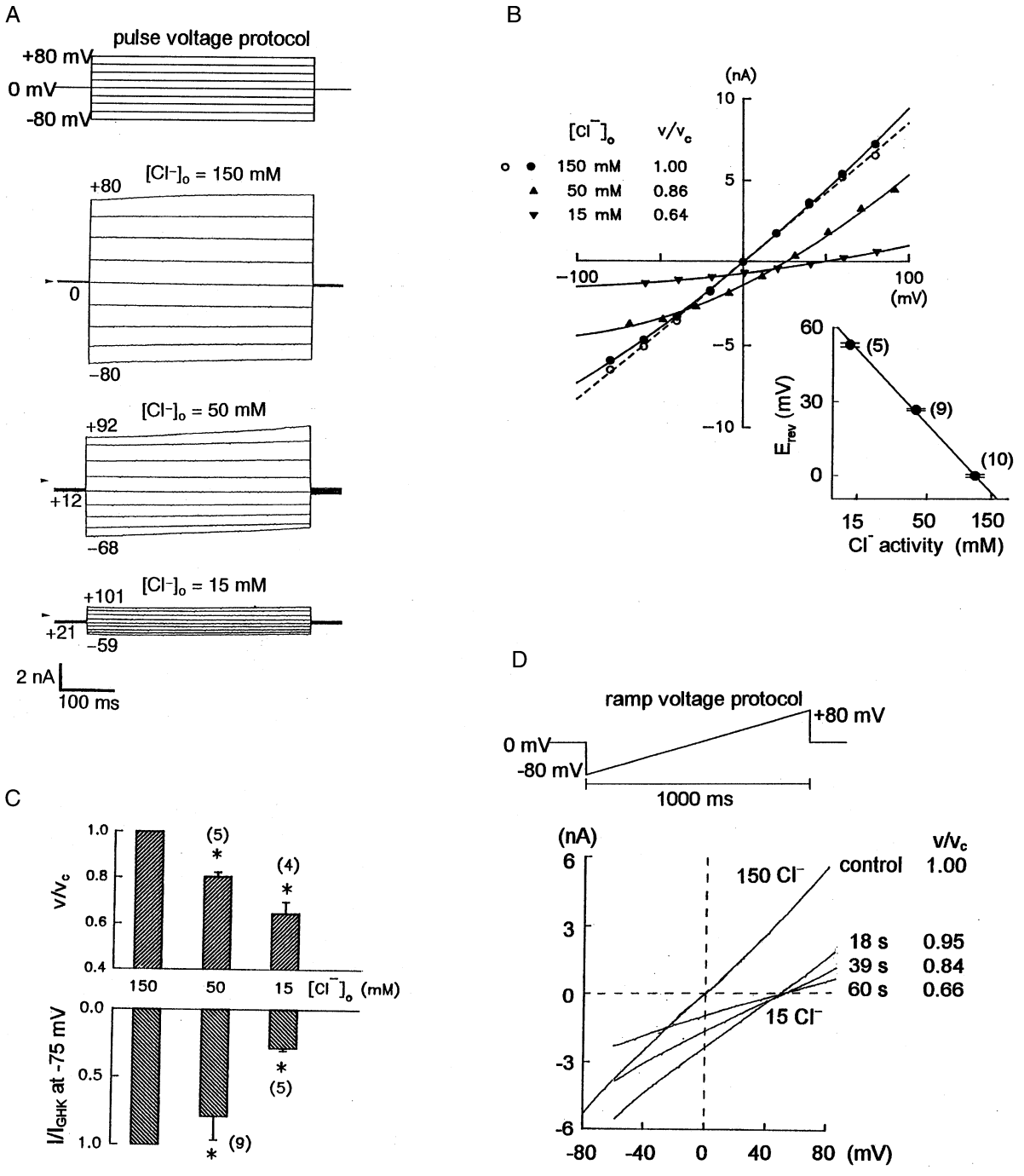

Fig. 2. Effects of reduced bath [Cl^-] on whole-cell current and cell volume. (*A*) Typical current responses to commands (at intervals of 1 sec) of voltage pulses (*top* panel) recorded from a cell for which the bathing solution was switched from solution E to solutions F and G sequentially. Current responses were recorded 1 min after each switching. To the left of current traces, holding potentials and the most positive and most negative pulse voltages, all corrected for liquid junction potentials, are indicated in mV. *Arrowheads*, zero-current level. (*B*) *I-V* curves derived from (*A*). *Filled* symbols, quasi-steady state current; *open* circles, instantaneous current. v/v_c, relative cell volume determined 1 min after each solution change. *Inset*, reversal potentials (E_{rev}) plotted against bath Cl^- activity. (*C*) Comparison of v/v_c and I/I_{GHK} as function of $[Cl^-]_o$, where I is current at −75 mV. *Asterisks*, statistically significant difference from control. In (*B*) and (*C*), vertical bars indicate ±SEM with the number of cells in parentheses. (*D*) Whole-cell *I-V* curves obtained by applying a ramp-voltage command (*top* panel) for control (solution E) and solution G. To the right of each curve, time after bath solution change and relative cell volume are indicated.

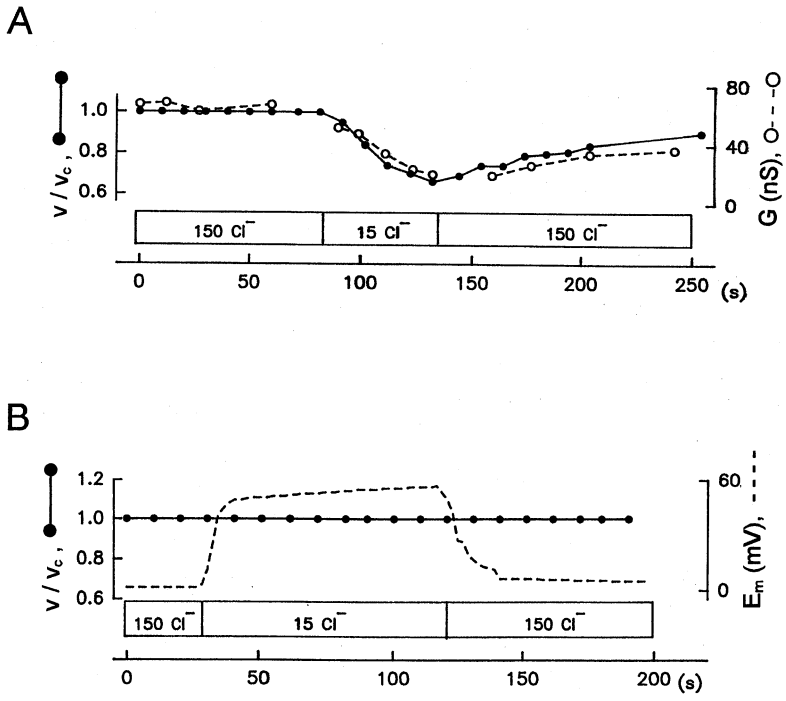

Fig. 3. Effects of reduced bath $[Cl^-]$ on relative cell volume (v/v_c) and whole-cell conductance (G): comparison between voltage- and current-clamp experiments. Bath was changed from solution E to solution G, then back to solution E. (*A*) Voltage-clamp experiment. *I-V* relations were obtained using the ramp-voltage protocol (Fig. 2*D*, top). (*B*) 'Zero-current' clamp experiment. Note constancy in v/v_c and changes in membrane potential (E_m) expected for a Cl^--selective membrane.

and almost faithfully reproduced the *I-V* relationships for the instantaneous current obtained with the pulse-voltage protocol (Fig. 2*B*).

Effect of Asymmetric $[Cl^-]$

Data from experiments with lowered bath Cl^- concentrations are also included in Fig. 2. Figure 2*B* shows *I-V* curves derived from the current traces in Fig. 2*A*. Values of E_{rev} varied by −58.6 mV per decade increase of Cl^- activity in the bath (Fig. 2*B*, *inset*); this slope approximated the Nernstian one (−59 mV/decade change of Cl^- activity) that applies to an ideally Cl^--selective membrane. Thus, the currents recorded from the isolated marginal cells are most likely Cl^- selective even though no compensation has been made for leakage currents. In addition, the fact that currents recorded at large negative membrane potentials apparently decreased with decreasing $[Cl^-]_o$ (Fig. 2*B*) raised the possibility that the $[Cl^-]_o$ had somehow affected the underlying permeability P_{Cl}.

To explore this possibility quantitatively, we calculated the ratio I/I_{GHK} (*see* Materials and Methods, Analysis) with the results presented in Fig. 2*C*. The ratio decreased systematically with lowerings of $[Cl^-]_o$, being correlated with reduction in cell volume. When the bath was switched from control (i.e., 150 mM Cl^-) to an isosmotic, low-Cl^- (15 mM) solution, E_{rev} shifted to a new level within 20 sec after switching and stayed there (Fig. 2*D*). In contrast, both the whole-cell conductance G and relative cell volume v/v_c continued to decline (Fig. 2*D*) and leveled off within 60 sec after switching. Figure 3*A* shows the result of a typical experiment to demonstrate these parallel changes in G and v/v_c. The close correlation between cell volume and Cl^- current thus suggested was further confirmed by clamping the cell to zero current (Fig. 3*B*). Under such a constraint the cell's initial volume persisted in the face of an intervening harsh change in $[Cl^-]_o$, as expected.

Anion Substitution

The dependence of whole-cell current on other anion species was examined by replacement of bath Cl^- with SCN^-, Br^-, F^-, NO_3^-, I^-, or gluconate$^-$ (all sodium salts at 150 mM). The results obtained are summarized in Figs. 4 and 5 and in Table 2. In this series of experiments, the ionic conditions employed were apparently asymmetric with respect to cation, namely, 140 mM $NMDG^+$ (pipette) *vs.* 150 mM Na^+ (bath). However, the outcome of this asymmetry was immaterial to the present study because the E_{rev}s observed for control (150 mM NaCl) averaged to near null or −1.2 ± 0.3 mV (N = 16), a value comparable to −0.4 ± 0.5 mV (N = 23) which was determined with 150 mM NMDG-Cl (solution E) in the bath. This finding indicates that the possible contribution of Na^+ conductance (more explicitly, P_{Na}) to membrane potential may be negligible compared with that of Cl^- conductance (or P_{Cl}) under the experimental conditions employed.

All the anions but Br^-, when substituted for bath Cl^-, caused a shift of E_{rev} (Fig. 4*B*). Values of E_{rev} and

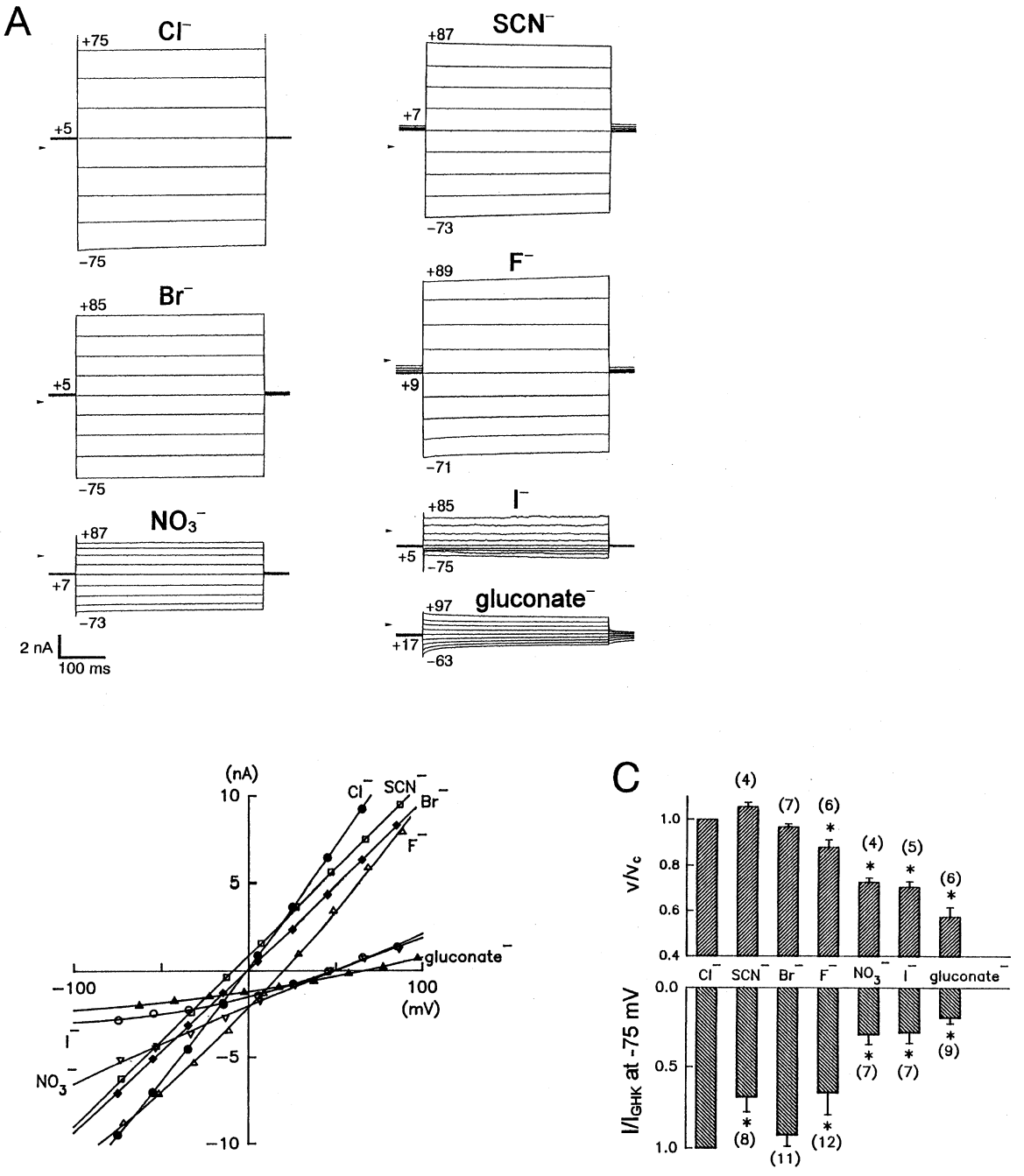

Fig. 4. Anion substitution study using the pulse-voltage protocol. (*A*) Current traces from a typical cell each recorded 1 min after bath solution change from control (solution D, $X = Cl^-$). *Arrowheads,* zero-current level. To the left of current traces, holding potentials and the most positive and most negative pulse voltages, corrected for liquid junction potentials, are indicated in mV. (*B*) *I-V* curves derived from quasi-steady state currents in (*A*). (*C*) Comparison of relative cell volume (v/v_c) and I/I_{GHK}, where *I* is current at −75 mV obtained 1 min after bath solution change. *Asterisks,* statistically significant difference from control. Vertical bars, ±SEM; number of cells in parentheses.

relative permeability (P_X/P_{Cl}) determined by applying the Goldman-Hodgkin-Katz voltage equation are listed in Table 2. The permeability sequence thus revealed was as $SCN^- > Br^- \cong Cl^- > F^- > NO_3^- \cong I^- >$ gluconate$^-$. After replacement of bath Cl^- by F^-, I^-, NO_3^- or gluconate$^-$ it took less than 20 sec for E_{rev} to attain a new level, which was stable and independent of changes in the cell volume and slope conductance (Fig. 5). But the anionic current and cell volume continued to decrease for an additional 40 sec or longer (Fig. 5). The E_{rev}s returned to control levels in about 20 sec after washout with 150 mM NaCl, while it took a few minutes for both

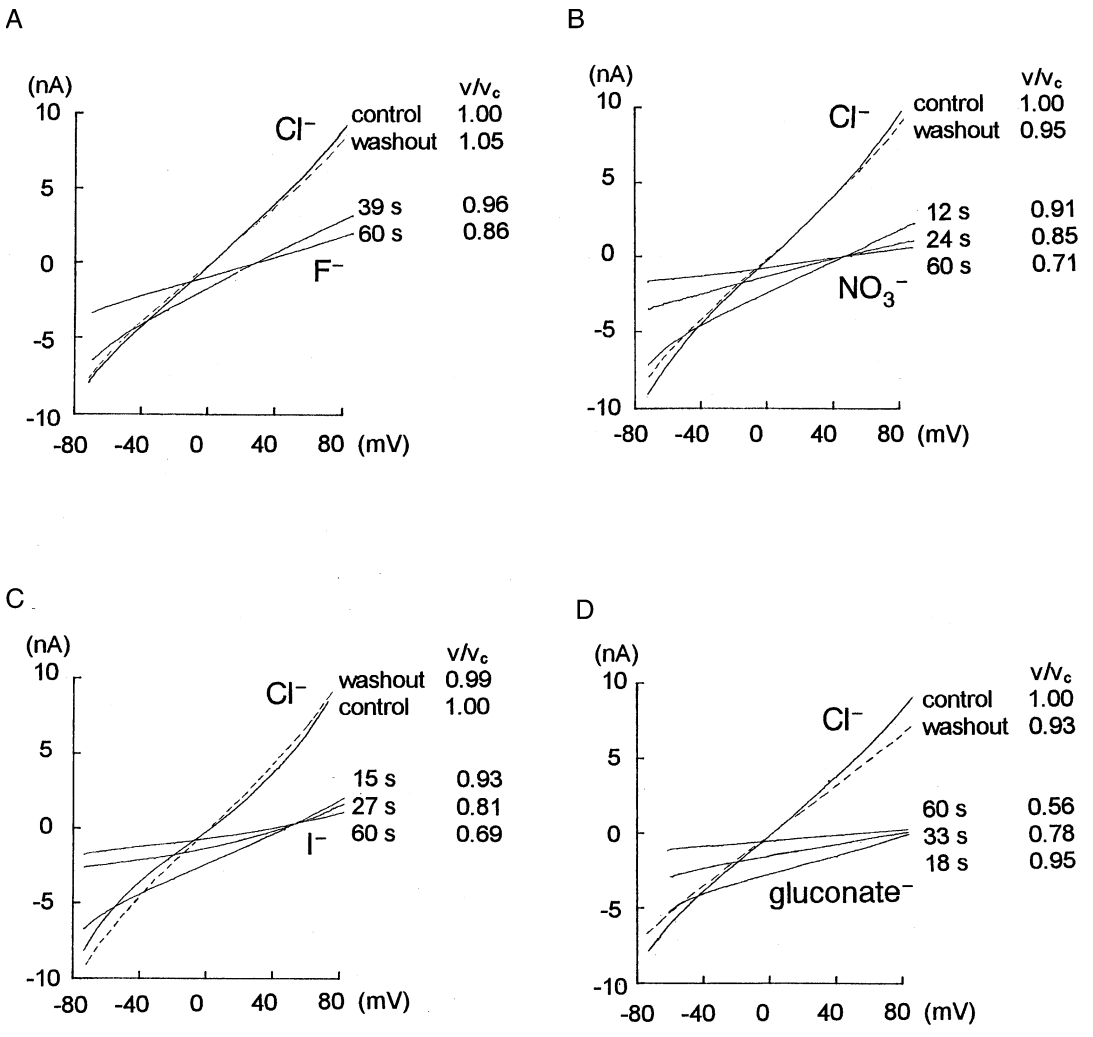

Fig. 5. Anion substitution study using the ramp-voltage protocol. *I-V* curves were recorded for control (solution D, $X = Cl^-$), anion substitution (solution D, $X = F^-$, NO_3^-, I^- or gluconate$^-$) and washout. Time after bath solution change and associated volume data are attached. Data for 'washout' were obtained 1.5 min after bath replacement.

Table 2. Reversal potentials (E_{rev}) for anion current under bi-ionic condition and derived permeabilities (P_x) relative to P_{Cl}

Anion	E_{rev} (mV)*	P_x/P_{Cl}	N
SCN^-	−7.5 ± 1.3	1.28	8
Br^-	−1.5 ± 0.3	1.01	12
Cl^-	−1.2 ± 0.3	1.00	16
F^-	+29.2 ± 2.7	0.31	13
NO_3^-	+54.0 ± 4.9	0.12	7
I^-	+58.8 ± 4.7	0.10	8
Gluconate$^-$	+93.9 ± 7.3	0.02	9

* Mean ± SEM. *N*, number of cells examined.

the cell volume and Cl^- current to recover (Fig. 5). These correlated changes in cell volume and anionic currents are summarized in Fig. 4*C* and appear to be consistent with the results from reduced $[Cl^-]_o$ (Fig. 2*C*). Finally, it should be noted that no significant changes in cell volume ensued following bath replacement by SCN^-, although the corresponding I/I_{GHK} ratio turned out to be significantly smaller than unity, a fact sharply contrasting to the other anions tested (Fig. 4*C*). This dissociation of cell volume and anionic current was not examined in detail in the present study.

Effect of Cl^- Channel Blockers

Bath application of DPC (1.0 mM) or NPPB (0.5 mM) suppressed the Cl^- current at both positive and negative membrane potentials (Fig. 6*A*). At a lower concentration neither DPC (0.1 mM, $N = 4$) nor NPPB (0.05 mM, $N = 4$) had any appreciable effect (*not shown*). Another blocker SITS was not effective even at a concentration as high as

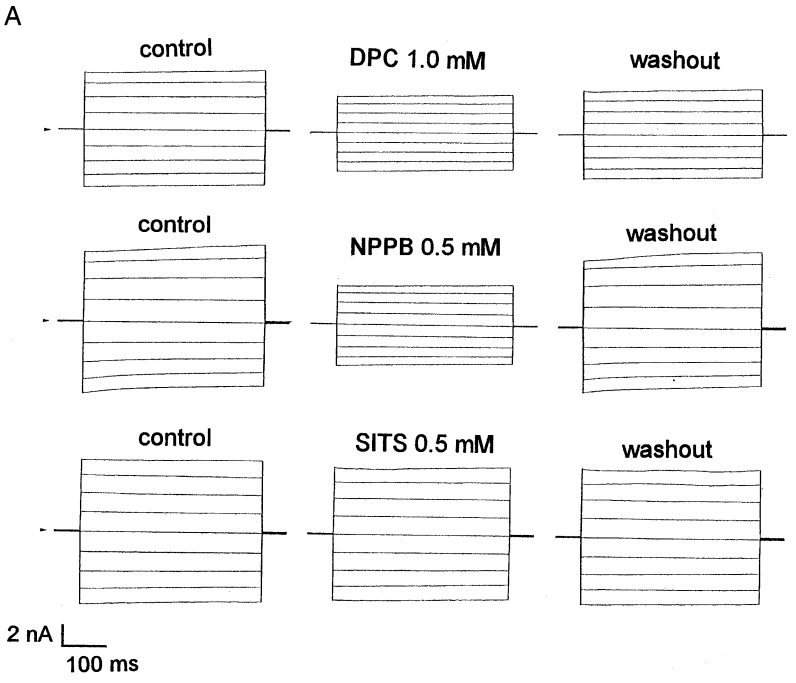

Fig. 6. Effects of Cl^- channel blockers. (*A*) Current traces obtained from the pulse-voltage protocol (Fig. 2*A*, *top*). Data were obtained 2 min after bath application of blockers. *Arrowheads*, zero-current level. (*B*) Slope conductance (*G*) at 0 mV. Data are normalized using mean values for control. *Asterisks*, statistically significant difference from control. Vertical bars, ± SEM; number of cells in parentheses.

0.5 mM. With the high doses of the effective blockers, the Cl^- currents were only partially inhibited, as shown in Fig. 6*B*, where the blocking efficiency was roughly 50% at most. None of these blockers, at the concentrations applied, exerted any detectable effect on cell volume.

Cell Volume Variation Induced by Altered Holding Potentials Under Isotonic Condition

When clamped to null potential under a quasi-symmetric Cl^- condition, cells did not appreciably change their volume for up to 5 min following formation of the whole-cell configuration. With the clamp voltage raised to +20 mV cells began to swell and resumed their original volume when released from the clamp voltage (Fig. 7*A*). Sustained clamping at +20 mV made the cell burst (*not shown*). Conversely, with the potential held at −35 mV, cell volume began to decrease and, upon release from the voltage, tended to recover toward the control level (Fig. 7*B*). Concomitantly with these time-dependent changes in cell volume the whole-cell conductance *G* also changed in parallel (Fig. 7). The mechanism of these volume changes will be detailed later.

Osmotic Challenge

To further characterize the volume-correlated Cl^- conductance, we subjected cells to hyper- or hyposmolalities that were adjusted with mannitol (solutions H, I, and K). As shown in Fig. 8*A* and *B*, the magnitude of the cell's current responses to the pulse-voltage commands increased or diminished systematically with varying osmo-

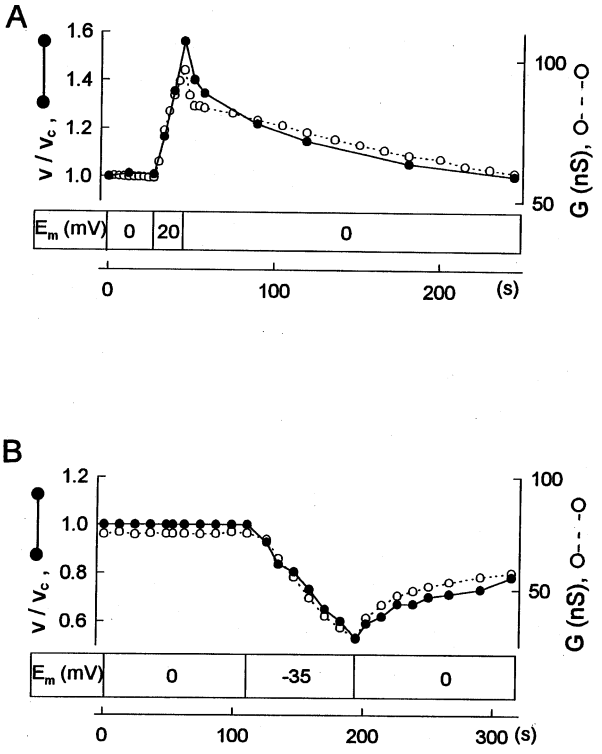

Fig. 7. Effects of sustained holding potential (E_m) on relative cell volume (v/v_c) and whole-cell conductance (G) for cells in quasi-symmetric Cl^-. The bath contained 150 mM NMDG-Cl (solution E). Cl^- conductance (G) was calculated by a linear fit to *I-V* relations obtained using the ramp-voltage protocol (Fig. 2*D*, *top*). Note parallel changes in v/v_c and G at both positive (*A*) and negative (*B*) intracellular potentials.

lalities. But the characteristics of the *I-V* relations, including their weak voltage and time dependency, were essentially the same under all the osmotic conditions tested. Time-chase experiments revealed that again the cell volume and conductance changed largely in parallel (Fig. 8*C* and *D*). The reason for small transient increases in G immediately after the onset of cell shrinkage (Fig. 8*C* and *D*, *arrows*) has not been clarified yet. The results of osmotic challenge leading to concomitant changes in both the volume and Cl^- conductance are summarized in Fig. 8*E*. The slope conductance G at 0 mV fell down to 31% of control (or ~5 nS/pF) at 448 mOsm/kg but still persisted against such a severe shrinkage.

Discussion

This paper is concerned with characterization of a novel Cl^- conductance detectable from marginal cells that were freshly isolated and subjected to various ionic or osmotic conditions. The major findings are summarized as: (i) a sizable *basal* whole-cell Cl^- conductance (~18 nS/pF) is operating in cells with normal shape and volume; (ii) its anion-selectivity sequence resembles that of a Cl^- channel previously found in the basolateral membrane of the same cell; (iii) this conductance varies in parallel with cell volume; (iv) the properties of the conductance differ, in many respects, from those described for other volume-sensitive Cl^- conductances and channels; and (v) least likely is that the cell volume perturbation has evoked a Cl^- conductance entirely different in origin from the observed *basal* conductance for Cl^-.

Similarity between the Whole-Cell Cl^- Conductance and the Cl^- Channel in Basolateral Membrane

Of the characteristics noted above, the selectivity sequence, P_{Cl} (1.00) ≅ P_{Br} (1.01) > P_F (0.31) > P_{NO_3} (0.12) ≅ P_I(0.10) (relative values in parentheses), is one of the salient features of the present Cl^- conductance. On the other hand, an 80-pS Cl^- channel found in the marginal cell's basolateral membrane (Takeuchi et al., 1995) has the following unique properties: (i) a linear *I-V* relationship for symmetrical Cl^-, (ii) a permeability sequence of P_{Cl} (1.00) ⩾ P_{Br} (0.90) > P_I (0.20) ⩾ P_{NO_3} (0.14), and (iii) no apparent voltage or time dependence. All these features resemble those of the whole-cell conductance, thus raising the possibility that a substantial fraction of the whole-cell current might be due to activation of the underlying Cl^- channels. The relatively high incidence (~60% of successful patches) of this channel type in the basolateral membrane, which comprises more than 80% of the total cell surface, also supports the above inference. The selectivity sequence, $Br^- \cong Cl^- > F^- > I^-$, presented here conforms to Eisenmann's sequence V, which implies that the Cl^- channel involved has relatively strong binding sites for anions (Wright & Diamond, 1977).

Compared to the 80-pS Cl^- channel, the whole-cell Cl^- current was less sensitive to DPC. The channel activity was fully blockable by DPC at 1 mM (Takeuchi et al., 1995), whereas, in the whole-cell current, the same concentration of blocker was only partially effective (Fig. 6). This apparent discrepancy could be explained if the blocker is more effective from the cytosolic side than from outside. The reason is as follows. In our previous single-channel studies with excised patches, that were mostly inside-out, the drug applied externally should have affected the channel activity primarily from the cytosolic side. In the present whole-cell study, by contrast, the primary site of action faced extracellularly indeed, though a certain fraction of DPC, a lipophilic acid, might have been acting from within the cell. In this regard, there is another possibility that an unspecified, intrinsic mechanism for channel activation could have been mobilized to attenuate the potency of the blocker down to the level observed here. The 80-pS Cl^- channel is insensitive to 1 mM DIDS (4,4′-diisothiocyanatostil-

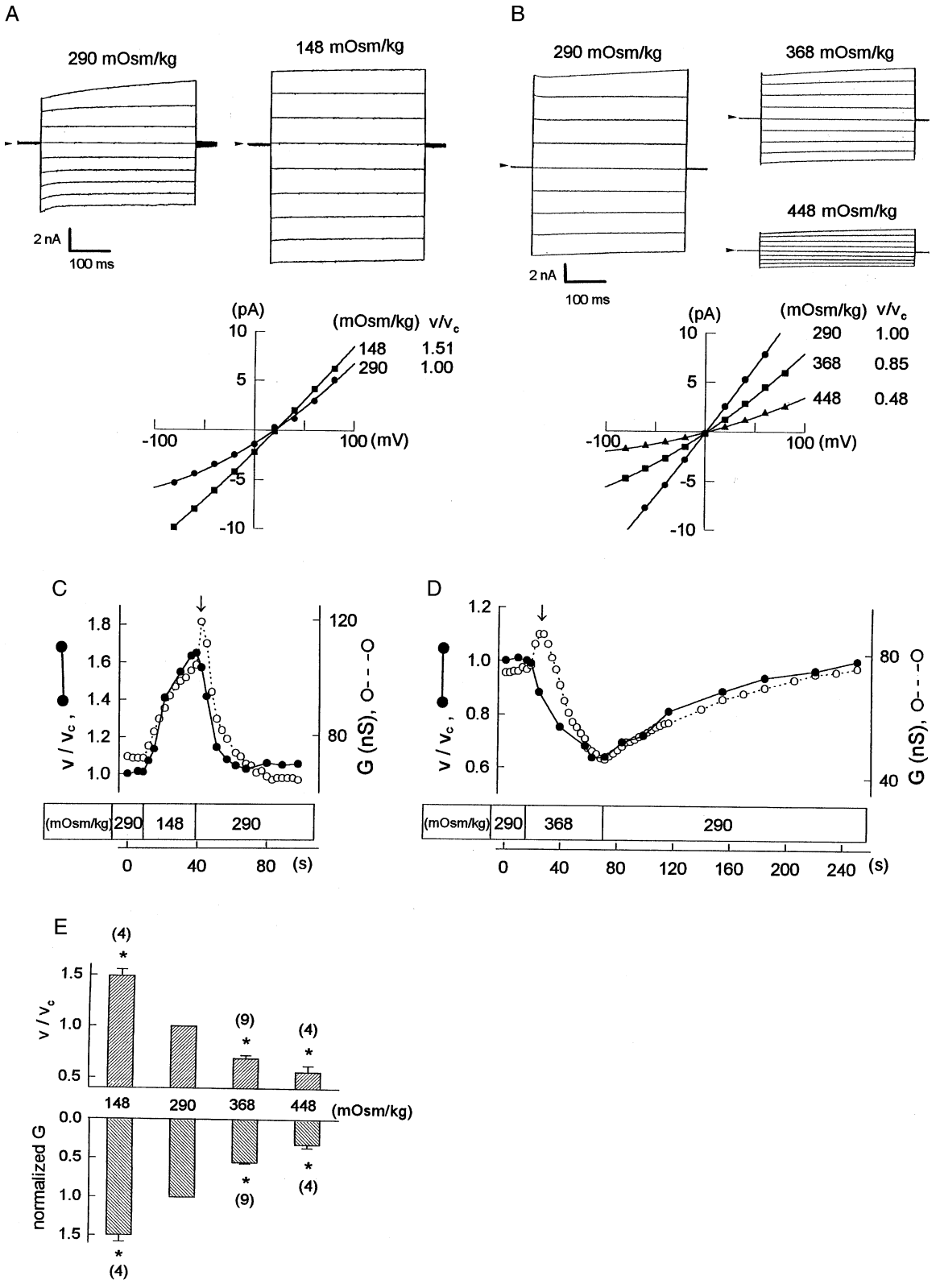

Fig. 8. Associated changes in cell volume (v/v_c) and Cl^- conductance (G) upon osmotic challenge. (*A*) and (*B*) Current recordings obtained using the pulse-voltage protocol (Fig. 2*A*, *top*) and derived *I-V* curves for quasi-steady state currents. *Arrows* indicate zero current level. In (*A*), the cell was bathed in solutions J and K sequentially and measured 0.5 min after solution change. In (*B*), the cell was bathed in solutions E, H and I sequentially and measured 2 min after each solution change. (*C*) and (*D*) Time course of changes followed using the ramp-voltage protocol. Note that both v/v_c and G calculated by a linear fit to *I-V* relations changed largely in parallel. (*E*) Comparison of v/v_c and normalized G as a function of osmolality. Data were obtained 0.5 min after bath solution change (hypotonic) or 2 min after (hypertonic). Control G values are 59.8 ± 6.4 nS ($N = 4$) for solution J (before hypotonic challenge) and 101.4 ± 8.1 nS ($N = 11$) for solution E (before hypertonic challenge). *Asterisks*, statistically significant difference from control. Vertical bars, ±SEM; number of cells in parentheses.

Table 3. Comparison with other volume-sensitive Cl^- conductances or channels

Origin or type	Selectivity	Rectification*	g (pS)**	Refs.†
Marginal cell				
Whole-cell conductance	$SCN^- > Br^- \cong Cl^- > F^- > NO_3^- \cong I^-$	Outward (weak)		This study
Basolateral Cl^- channel***	$Cl^- > Br^- > I^- \geqslant NO_3^-$	No	~80	1
Swelling-activated conductance				
Group I	$I^- > Br^- > Cl^- > F^-$	Outward, time independent		2,3
Group II	$SCN^- > I^- \geqslant Br^- > Cl^- > F^-$	Outward, time dependent	30–50	4–9
Group III	$NO_3^- \geqslant Br^- \cong Cl^- \cong F^- \cong I^-$	Outward	<10	10–13
Channel				
ClC-2	$Cl^- \geqslant Br^- > I^-$	No	3–5	14–16
Large-conductance Cl^-			300–400	17

* Observed for steady-state currents. ** Single channel conductance. *** Volume-sensitivity is not studied.
† (1) Takeuchi et al., 1995, (2) Tseng, 1992, (3) Pollard, 1993, (4) Worrel et al., 1989, (5) Solc & Wine, 1991, (6) Kubo & Okada, 1992, (7) Chan et al., 1993, (8) Diaz et al., 1993, (9) Okada et al., 1994, (10) Cahalan & Lewis, 1988, (11) Christensen & Hoffmann, 1992, (12) Doroshenko & Neher, 1992, (13) Stoddard et al., 1993, (14) Thiemann et al., 1992, (15) Gründer et al., 1992, (16) Jentsch, 1994, (17) Falke & Misler, 1989.

bene-2,2′-disulfonic acid) (Takeuchi et al., 1995); however, its insensitivity to SITS has not been reported thus far.

Comparison with Other Work

A variety of Cl^- conductances and channels are known to be volume sensitive, or rather, some of them are postulated to play an essential role in the regulation of cell volume. For comparison, such conductances and channels of immediate concern are summarized in Table 3. Among these, the ClC-2 has a selectivity sequence similar to the one we have determined in this and previous studies. However, a naive analogy between the ClC-2 and our 80-pS Cl^- channel should be avoided since the ClC-2 is activated only upon hyperpolarization or swelling of the cell. The single-channel conductance is another discriminant between the two.

The present Cl^- conductance is featured by its relatively large size (~18 nS/pF), which was patent in nonswollen cells. Further, even after a hypertonic shrinkage down to ~60% of the control, a sizable conductance of ~5 nS/pF still persisted (Fig. 8). The majority of known volume-sensitive Cl^- conductances are activated by cell swelling under a hypotonic stress (Cahalan & Lewis, 1988; Worrel et al., 1989; Kubo & Okada, 1992; Tseng, 1992; Banderali & Roy, 1992; Pollard, 1993; Chan et al., 1993; Diaz et al., 1993). As an interesting exception to this, Jackson & Strange (1993) have reported on a volume-sensitive Cl^- conductance of 1.5-2 nS/pF in isosmotically swollen cells; this conductance, however, tends to null (~0.02 nS/pF) upon exposure to ~440 mOsm.

A weak dependence on both voltage and time is another characteristic of the volume-dependent Cl^- conductance in the marginal cell. The Cl^- currents termed Group I (Table 3) are induced by cell swelling and independent of time also, but their voltage dependence and ion selectivity are both at variance with ours. Cl^- conductances (G) categorized as Group II (Table 3), on the other hand, share several common characteristics with each other. These include: (i) small or negligible G values in cells with normal volume, (ii) apparent increases of G concomitant with cell swelling, (iii) a selectivity sequence of $I^- \geqslant Br^- > Cl^- > F^-$, (iv) sensitivity to DPC, SITS and NPPB, (v) outward rectification, and (vi) time-dependent inactivation at large positive membrane potentials. An intermediate-sized (30–50 pS) unitary conductance with its dependence on voltage and time is also a characteristic of the single-channel events associated with the Cl^- currents of Group II (Solc & Wine, 1991; Okada et al., 1994). Accordingly, the marginal cell's Cl^--selective conductance and channel differ, in many respects, from the Group II conductances. Channels in Group III have relatively small (<10 pS) unitary conductances; more importantly, they poorly discriminate among halides (Cahalan & Lewis, 1988; Stoddard et al., 1993). A large-conductance (300–400 pS) Cl^- channel from neuroblastoma cells is documented (Falke & Misler, 1989). However, other discriminants such as the selectivity sequence are unknown for this channel. In summary, we could not find any comparable volume-sensitive Cl^- conductances in the literature.

Finally, comparison is made with other Cl^- channels for which the volume sensitivity is unknown. In the apical membrane of marginal cells, Sunose et al. (1993) have found a cyclic AMP-dependent, nonrectifying, small-g-value Cl^- channel, which is similar to the cystic fibrosis transmembrane regulator (CFTR). It is unlikely that the whole-cell Cl^- current here concerned depends

heavily on the activity of this channel type because no particular maneuver was employed to elevate the cyclic AMP level in our cells and because the selectivity sequence ($Br^- \geqslant Cl^- > I^- > F^-$) reported for the CFTR (for review, *see* Welsh et al., 1994) differs from that of the present Cl^- conductance. The ClC-K1 channel displays a selectivity sequence of $Br^- > Cl^- > I^-$, weak outward rectification and no apparent time dependence (Uchida et al., 1993). These features are shared by our Cl^- conductance indeed, but whether or not the volume correlation is also a common characteristic between the two remains open at present. Likewise, in light of their ion selectivity, voltage dependency and other properties, none of the following channels can be a likely candidate that accounts for the Cl^- conductance of marginal cells: (i) the outwardly-rectifying Ca^{2+}-activated channel (Marty, Tan & Trautmann, 1984; Evans & Marty, 1986; Cliff & Frizzell, 1990; Gray et al., 1994), (ii) the outwardly-rectifying channel with an intermediate *g*-value (Halm et al., 1988; Li, McCann & Welsh, 1990), (iii) ClC-0 (for review, *see* Jentsch, 1994), and (iv) ClC-1 (Steinmeyer, Ortland & Jentsch, 1991).

Correlation with Cell Volume

Under the conditions employed, the variation of Cl^- conductance was closely associated with that of cell volume. In light of the facts that the *I-V* relations showed similar characteristics under all the osmotic conditions tested (Fig. 8*A* and *B*) and that the E_{rev} level for each anion species was not affected by the changes in cell volume (Fig. 5), we consider that the major component of the Cl^- currents observed here originated from the same type of Cl^- conductance. A question arises: Which of the two, volume or conductance, is the cause of the other? In the case of osmotic challenge with mannitol (Fig. 8), the resulting shrinkage or swelling of cells can be the primary cause of subsequent changes in conductance. In experiments employing reduced bath Cl^- strengths (Fig. 2), anion substitution (Figs. 4 and 5), and nonzero holding potentials (Fig. 7), on the other hand, the cell volume changed even in the absence of any appreciable osmotic imbalance across the membrane. However, in these latter cases also, Cl^- currents forced by the imposed electrochemical potential gradients did cause a net solute loss or gain, both giving rise to an obligatory flux of water. A simplified model for this situation, inclusive of its outcome, is presented below.

Suppose that a cell with a membrane predominantly Cl^--selective is giga-sealed onto a micropipette containing isotonic buffer whose principal ions are $NMDG^+$ and Cl^- and that the cell interior has already been dialyzed against a much larger volume of pipette solution. Upon injection of an inward current, for instance, a net efflux of Cl^- should cross the membrane, and, at the pipette opening also, both a net influx of Cl^- and a net efflux of

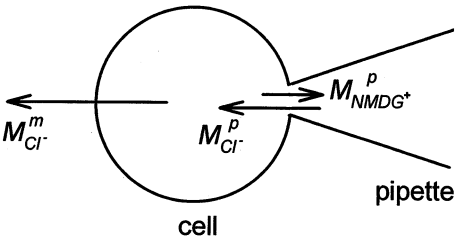

Fig. 9. Illustration of a mechanism for volume changes due to whole-cell voltage-clamping. M_i, flux of ion *i* across cell membrane (*m*) or pipette tip (*p*). Given a cell with ideally Cl^--selective membrane, the whole-cell current across the membrane is carried by Cl^- exclusively, while at the pipette tip the same current is shared by both Cl^- and $NMDG^+$. From this asymmetry would ensue a net loss or gain of cell osmolytes depending on the direction of membrane current (*see* text).

$NMDG^+$ are expected to occur (Fig. 9). For such fluxes, the mass balance equation may be written, from the continuity of current, as

$$M^m_{Cl} = M^p_{Cl} + M^p_{NMDG}, \tag{3}$$

where M_i is the *scalar* net flux of ion *i* across membrane (*m*) or pipette tip (*p*). Introducing $\alpha = M^p_{NMDG}/M^p_{Cl}$ we can rewrite Eq. (3) into

$$M^m_{Cl} = (1 + \alpha)M^p_{Cl}. \tag{4}$$

Then, the net solute *loss* from cell per unit time, ΔM, is given by

$$\Delta M = M^m_{Cl} + M^p_{NMDG} - M^p_{Cl} = 2\alpha M^p_{Cl}, \tag{5}$$

which is positive since $\alpha > 0$ by definition. Consequently, upon injection of an inward current, the cell would certainly shrink until the net loss of osmolytes is fully counterbalanced by buffering with the pipette solution.

By way of example, a numerical assessment is made of the data in Fig. 7*B*, where a certain net amount of charges escaped from the cell as a result of voltage clamping at −35 mV for 80 sec (=*T*). The net amount of Cl^- ions that left the cell toward the extracellular bulk during the period of voltage clamp (i.e., $\int_0^T M^m_{Cl}\, dt$) is estimated to be 1.5 pmol (*see* Appendix A). Then, from Eqs. (4) and (5), together with a reasonable assumption that $\alpha = 0.3$ (*see* Appendix B), we obtain a value of 0.7 pmol for a net loss of cell ions (i.e., $\int_0^T \Delta M\, dt$). This much solute loss, in turn, may well drag cell water out by 2.3 pl, under the constraint of isotonicity throughout the measurements. On the other hand, the cell volume is estimated to be ~1.6 pl when assuming a cylinder 10 μm wide by twice that long (*cf.* Fig. 1*A*). This is a volume comparable to the dragged water volume, or even less; therefore, the cell should have been deprived of water within 1 min unless properly supplied with the pipette solution. That the shrinkage of the present cell remained

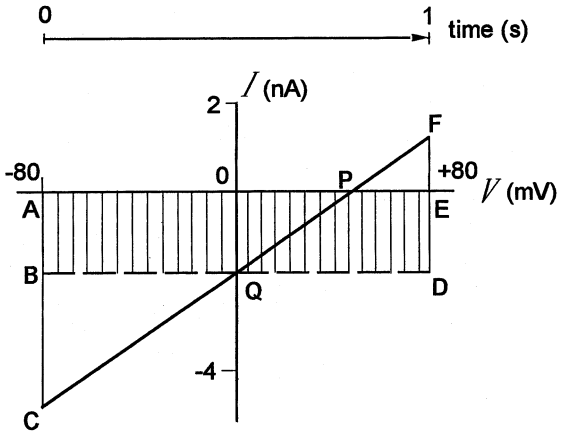

Fig. 10. Schematic drawing of the *I-V* relation obtained by applying the ramp-voltage command (Fig. 2*D*, *top*) to a cell bathed in 15 mM Cl^- solution. P, reversal potential; Q, current level corresponding to 'zero' holding potential. Note that the shaded rectangle (□ ABDE), which represents the amount of charges displaced by clamping the cell for 1 sec at 'zero' holding potential, has an area equal to the area for Δ ACP *minus* Δ FPE.

at a level as moderate as ~40% (Fig. 7*B*) indicates the validity of the above interpretation. The use of pipettes with relatively small openings (3–5 MΩ) in this study must have retarded diffusion across the pipette tip significantly, thereby rendering the current-induced volume changes manifest. This is an example of electro-osmosis at the single cell level. A similar volume change has been reported for the hair cell (Iwasa, 1995). However, in most of the whole-cell patch clamp experiments reported so far, cell volume changes as a result of current passing have been rarely detectable probably because of a relative weakness of the responsible ionic current.

It appears pertinent to point out that the frequency of voltage ramps (Fig. 2*D*, *top*) as applied to the cell under asymmetric Cl^- conditions does not modify the intrinsic trend of cell volume change. As an example, we shall consider current responses presented in Fig. 2*D*, *bottom*. Here, the *I-V* curves are almost linear, and the current levels for $V = 0$ (holding potential) are negative throughout. How many charges should have moved during a single sweep of voltage ramp (i.e., 1 sec)? As illustrated in Fig. 10, the amount of displaced charges is defined as the area demarcated by the slope line and the abscissa; thus the net outward movement of charges, more specifically, of Cl^- ions in this particular case, may be given by the difference in area between the two triangles depicted in Fig. 10. Note also that the exactly same amount of net charges should cross the membrane irrespective of the frequency of ramp cycles, as far as the holding potential is set at 0 mV.

In any case, the observed parallel changes in Cl^- conductance and cell volume appear to be of autocatalytic nature; that is to say, an imposed membrane stretch or a perturbation in the cytoskeletal system by cell swelling, for instance, may lead to an increase in *G* by way of recruiting dormant Cl^- channels or by activation of the underlying 80-pS Cl^- channels at 'substate' (Takeuchi et al., 1995) to their 'full-open' state. Such an augmented Cl^- flux, in turn, is expected to further add to cell volume. There are, however, some other possibilities that the Cl^- flux itself may have directly induced changes in conductance and that voltage-dependent activation or inactivation of the underlying Cl^- channels could also have contributed, to some extent, to the conductance changes observed.

Physiological Relevance

There is morphological as well as electrophysiological evidence that the Na-K-2Cl cotransporter functions in the strial marginal cells (Quick & Duvall, 1970; Kusakari et al., 1978; Rybak & Morizono, 1982). Under physiological conditions, a net influx of ions via this route could induce an influx of water, leading to an eventual increase in cell volume. However, the electroneutral nature of this cotransporter precludes its direct involvement in the observed cell volume changes that are closely associated with Cl^- current. As in many other animal cells, the volume-correlated Cl^- conductance here reported may play an important role in the volume regulation, though not yet established in the marginal cell. The conductance value as large as ~18 nS/pF in non-swollen cells, a salient feature of the present Cl^- conductance, may be related to the possible high rate of Cl^- influx via the postulated Na-K-2Cl cotransporters. The involvement of this cotransporter will be dealt with in a separate paper. The large Cl^- conductance, which probably has its origin in the basolateral membrane, may play an essential role in the generation of transepithelial potential difference across the layer of marginal cells, as suggested by Wangemann et al. (1995) and Takeuchi et al. (1995). In addition, an efflux of Cl^- via the relevant Cl^- conductance may depolarize the cell, leading to activation of the voltage-dependent K^+ channels in the apical membrane of marginal cells (Sunose et al., 1994). The Cl^- conductance, through its correlation with cell volume, might serve as a moderator for the inward or outward transfer of this anion. On the other hand, despite the lack of evidence for any volume-sensitive cation conductance in the marginal cell, it is still conceivable that, in the volume regulation of this particular cell type, the Cl^- conductance reported here may function in concert with the Ca^{2+}-activated nonselective cation channels that have been recently found in both the apical and basolateral membranes of the same cell (Takeuchi et al., 1992; Sunose et al., 1993; Takeuchi et al., 1995), in case the marginal cell has a swelling-triggered mechanism of $[Ca^{2+}]_i$ elevation, as reported for a human epithelial cell

line (Hazama & Okada, 1990). The molecular mechanism underlying such an interesting function awaits further studies.

The authors wish to thank Dr. Daniel C. Marcus, Boys Town National Institute, Omaha, NE, for his helpful comments. This study was supported in part by a grant (#06771417) from The Ministry of Education, Science and Culture, Japan.

References

Banderali, U., Roy, G. 1992. Activation of K^+ and Cl^- channels in MDCK cells during volume regulation in hypotonic media. *J. Membrane Biol.* **126:**219–234

Cahalan, M.D., Lewis, R.S. 1988. Role of potassium and chloride channels in volume regulation by T lymphocytes. *In:* Cell Physiology of Blood. R.B. Gunn and J.C. Parker, editors. pp. 281–301. Rockefeller University, New York

Chan, H.C., Fu, W.O., Chung, Y.W., Huang, S.J., Zhou, T.S., Wong, P.Y.D. 1993. Characterization of a swelling-induced chloride conductance in cultured rat epididymal cells. *Am. J. Physiol.* **265:** C997–C1005

Christensen, O., Hoffmann, E.K. 1992. Cell swelling activates K^+ and Cl^- channels as well as nonselective, stretch-activated cation channels in Ehrlich ascites tumor cells. *J. Membrane Biol.* **129:**13–36

Cliff, W.H., Frizzell, R.A. 1990. Separate Cl^- conductances activated by cAMP and Ca^{2+} in Cl^- secreting epithelial cells. *Proc. Natl. Acad. Sci. USA* **87:**4956–4960

Díaz, M., Valverde, M.A., Higgins, C.F., Rucareanu, C., Sepúlveda, F.V. 1993. Volume-activated chloride channels in HeLa cells are blocked by verapamil and dideoxyforskolin. *Pfluegers Arch.* **422:**347–353

Doroshenko, P., Neher, E. 1992. Volume-sensitive chloride conductance in bovine chromaffin cell membrane. *J. Physiol.* **449:**197–218

Evans, M.G., Marty, A. 1986. Calcium-dependent chloride currents in isolated cells from rat lacrimal glands. *J. Physiol.* **378:**437–460

Falke, L.C., Misler, S. 1989. Activity of ion channels during volume regulation by clonal N1E115 neuroblastoma cells. *Proc. Natl. Acad. Sci. USA* **86:**3919–3923

Gray, M.A., Winpenny, J.P., Porteous, D.J., Dorin, J.R., Argent, B.E. 1994. CFTR and calcium-activated chloride currents in pancreatic duct cells of a transgenic CF mouse. *Am. J. Physiol.* **266:**C213–C221

Gründer, S., Thiemann, A., Pusch, M., Jentsch, T.J. 1992. Regions involved in the opening of ClC-2 chloride channel by voltage and cell volume. *Nature* **360:**759–762

Halm, D.R., Rechkemmer, G.R., Schoumacher, R.A., Frizzell, R.A. 1988. Apical membrane chloride channels in a colonic cell line activated by secretory agonists. *Am. J. Physiol.* **254:**C505–C511

Hazama, A., Okada, Y. 1990. Involvement of Ca^{2+}-induced Ca^{2+} release in the volume regulation of human epithelial cells exposed to a hypotonic medium. *Biochem. Biophys. Res. Comm.* **167:**287–293

Iwasa, K.H. 1995. Membrane motor in the outer hair cell of the mammalian ear. *Comments Theoret. Biol.* (*in press*)

Jackson, P.S., Strange, K. 1993. Volume-sensitive anion channels mediate swelling-activated inositol and taurine efflux. *Am. J. Physiol.* **265:**C1489–C1500

Jentsch, T.J. 1994. Molecular biology of voltage-gated chloride channels. *In:* Chloride Channels. W.B. Guggino, editor. pp. 35–57. Academic, San Diego

Johnstone, B.M., Sellick, P.M. 1972. The peripheral auditory apparatus. *Quart. Rev. Biophys.* **5:**1–57

Kubo, M., Okada, Y. 1992. Volume-regulatory Cl^- channel currents in cultured human epithelial cells. *J. Physiol.* **456:**351–371

Kusakari, J., Ise, I., Comegys, T.H., Thalmann, I., Thalmann, R. 1978. Effect of ethacrynic acid, furosemide, and ouabain upon the endolymphatic potential and upon high energy phosphates of the stria vascularis. *Laryngoscope* **88:**12–37

Li, M., McCann, J.D., Welsh, M.J. 1990. Apical membrane Cl^- channels in airway epithelia: anion selectivity and effect of an inhibitor. *Am. J. Physiol.* **259:**C295–C301

Marty, A., Neher, E. 1983. Tight-seal whole-cell recording. *In:* Single channel recording. B. Sakmann, E. Neher, editors. pp. 107–122. Plenum, New York

Marty, A., Tan, Y.P., Trautmann, A. 1984. Three types of calcium-dependent channel in rat lacrimal glands. *J. Physiol.* **357:**293–325

McCann, J.D., Li, M., Welsh, M.J. 1989. Identification and regulation of whole-cell chloride currents in airway epithelium. *J. Gen. Physiol.* **94:**1015–1036

Okada, Y., Petersen, C.C.H., Kubo, M., Morishima, S., Tominaga, M. 1994. Osmotic swelling activates intermediate-conductance Cl^- channels in human intestinal epithelial cells. *Jpn. J. Physiol.* **44:**403–409

Pollard, C.E. 1993. A volume-sensitive Cl^- conductance in a mouse neuroblastoma × rat dorsal root ganglion cell line (F11). *Brain Res.* **614:**178–184

Quick, C., Duvall, A. 1970. Early changes in the cochlear duct from ethacrynic acids: an electron microscope evaluation. *Laryngoscope* **80:**954–960

Robinson, R.A., Stokes, R.H. 1968. The limiting mobilities of ions. *In:* Electrolyte Solutions. R.A. Robinson and R.H. Stokes, editors. pp. 118–132. Butterworths, London

Rybak, L.P., Morizono, T. 1982. Effect of furosemide upon endolymph potassium concentration. *Hearing Res.* **7:**223–231

Solc, C.K., Wine, J.J. 1991. Swelling-induced and depolarization-induced Cl^- channels in normal and cystic fibrosis epithelial cells. *Am. J. Physiol.* **261:**C658–674

Steinmeyer, K., Ortland, C., Jentsch, T.J. 1991. Primary structure and functional expression of a developmentally regulated skeletal muscle chloride channel. *Nature* **354:**301–304

Stoddard, J.S., Steinbach, J.H., Simchowitz, L. 1993. Whole cell Cl^- currents in human neutrophils induced by cell swelling. *Am. J. Physiol.* **265:**C156–C165

Sunose, H., Ikeda, K., Saito, Y., Nishiyama, A., Takasaka, T. 1993. Nonselective cation and Cl channels in luminal membrane of the marginal cell. *Am. J. Physiol.* **265:**C72–C78

Sunose, H., Ikeda, K., Suzuki, M., Takasaka, T. 1994. Voltage-activated K channel in luminal membrane of marginal cells of stria vascularis dissected from guinea pig. *Hearing Res.* **80:**86–92

Takeuchi, S., Ando, M., Kozakura, K., Saito, H., Irimajiri, A. 1995. Ion channels in basolateral membrane of marginal cells dissociated from gerbil stria vascularis. *Hearing Res.* **83:**89–100

Takeuchi, S., Irimajiri, A. 1995. Volume-dependent Cl^- conductance of the marginal cell and maxi-K^+ channels in the plasma membrane of the basal cell. *Assoc. Res. Otolaryngol.* **18:**26*A* (*Abstr.*)

Takeuchi, S., Marcus, D.C., Wangemann, P. 1992. Ca^{2+}-activated nonselective cation, maxi K^+ and Cl^- channels in apical membrane of marginal cells of stria vascularis. *Hearing Res.* **61:**86–96

Thiemann, A., Gründer, S., Pusch, M., Jentsch, T.J. 1992. A chloride channel widely expressed in epithelial and non-epithelial cells. *Nature* **356:**57–60

Tseng, G.N. 1992. Cell swelling increases membrane conductance of canine cardiac cells: evidence for a volume-sensitive Cl channel. *Am. J. Physiol.* **262:**C1056–C1068

Uchida, S., Sasaki, S., Furukawa, T., Hiraoka, M., Imai, T., Hirata, Y., Marumo, F. 1993. Molecular cloning of a chloride channel that is

regulated by dehydration and expressed predominantly in kidney medulla. *J. Biol. Chem.* **268:**3821–3824

Wangemann, P., Liu, J., Marcus, D.C. 1995. Ion transport mechanisms responsible for K^+ secretion and the transepithelial voltage across marginal cells of stria vascularis in vitro. *Hearing Res.* **84:**19–29

Wangemann, P., Marcus, D.C. 1992. The membrane potential of vestibular dark cells is controlled by a large Cl^- conductance. *Hearing Res.* **62:**149–156

Welsh, M.J., Anderson, M.P., Rich, D.P., Berger, H.A., Sheppard, D.N. 1994. The CFTR chloride channel. *In:* Chloride Channels. W.B. Guggino, editor. pp. 153–171. Academic, San Diego

Worrell, R.T., Butt, A.G., Cliff, W.H., Frizzell, R.A. 1989. A volume-sensitive chloride conductance in human colonic cell line T84. *Am. J. Physiol.* **256:**C1111–C1119

Wright, E.M., Diamond, J.M. 1977. Anion selectivity in biological systems. *Physiol. Rev.* **57:**109–156

Appendix A

Estimation of Net Outward Movement of Cl^- across Membrane for Data in Figure 7B

Suppose a net amount of charges (Q) carried by M^m_{Cl} over a period of 80 sec (=T), during which the imposed clamp voltage (V) of −35 mV has induced a time-dependent Cl^- current $I(t)$, or alternatively, conductance $G(t)$. Then, Q is given by

$$Q = \int_0^T I(t)dt$$

$$= \int_0^T VG(t)dt. \quad \text{(A1)}$$

As the experiment shows that $G(t)$ is a quasi-linear function of time, Q is readily obtained, through integration of Eq. (A1), as 147 nC. Division of this value by F (=96,500 C mol^{-1}) yields

$$\int_0^T M^m_{Cl}\, dt = 1.5 \text{ pmol.} \quad \text{(A2)}$$

Appendix B

Estimation of α for NMDG-Cl Solution

The parameter α (=M^p_{NMDG}/M^p_{Cl}) is also defined as a ratio of transference numbers, t_{NMDG^+} and t_{Cl^-}:

$$\alpha = t_{NMDG^+}/t_{Cl^-}. \quad \text{(A3)}$$

To the authors' knowledge, however, values of ts for isotonic aqueous NMDG-Cl are lacking. So we have estimated α by assuming

$$t_{NMDG^+}/t_{Cl^-} = \lambda_{0\,NMDG^+}/\lambda_{0\,Cl^-}, \quad \text{(A4)}$$

where λ_0 is limiting equivalent conductivity for the specified ion. The value of λ_0 for $NMDG^+$ (M.W. 195) is calculated to be 22.7 S cm^2 $equiv^{-1}$ by interpolation between the λ_0 values for two organic cations of near sizes. These are: λ_0 for $N(C_3H_7)_4^+$ (M.W. 186) = 23.4 S cm^2 $equiv^{-1}$ and λ_0 for $N(C_4H_9)_4^+$ (M.W. 242) = 19.4 S cm^2 $equiv^{-1}$ (Robinson & Stokes, 1968). The $\lambda_{0\,Cl^-}$ (=76.35 S cm^2 $equiv^{-1}$) is also available in the same reference, so that from Eqs. (A3) and (A4) we have obtained α = 0.3.